Polymer 50 (2009) 6202–6211

Contents lists available at ScienceDirect

Polymer

journal homepage: www.elsevier.com/locate/polymer

Functionalized organic nanoparticles from core-crosslinked poly(4-vinylbenzocyclobutene-*b*-butadiene) diblock copolymer micelles

Georgios Sakellariou [a], Apostolos Avgeropoulos [b], Nikos Hadjichristidis [c], Jimmy W. Mays [a,d,*], Durairaj Baskaran [a,*]

[a] Department of Chemistry, University of Tennessee, Knoxville, TN 37996, USA
[b] Department of Materials Science and Engineering, University of Ioannina Administration Building, University Campus Dourouti, 45110 Ioannina, Greece
[c] Department of Chemistry, University of Athens,Panepistimiopolis Zografou, 15771 Athens, Greece
[d] Chemical Sciences Division and Center for Nanophase Materials Sciences, Oak Ridge National Laboratory, Oak Ridge, TN 37831, USA

ARTICLE INFO

Article history:
Received 2 September 2009
Received in revised form
14 October 2009
Accepted 15 October 2009
Available online 22 October 2009

Keywords:
Nanoparticles
Surface-functionalization
Diblock copolymers

ABSTRACT

Surface-functionalized polymeric nanoparticles were prepared by: a) self-assembly of poly(4-vinylbenzocyclobutene-*b*-butadiene) diblock copolymer (PVBCB-*b*-PB) to form spherical micelles (diameter: 15–48 nm) in decane, a selective solvent for PB, b) crosslinking of the PVBCB core through thermal dimerization at 200–240 °C, and c) cleavage of the PB corona via ozonolysis and addition of dimethyl sulfide to afford aldehyde-functionalized nanoparticles (diameter: ~16–20 nm), along with agglomerated nanoparticles ranging from ~30 to ~100 nm in diameter. The characterization of the diblock copolymer precursors, the intermediate micelles and the final surface-functionalized crosslinked nanoparticles was carried out by a combination of size exclusion chromatography, static and dynamic light scattering, viscometry, thermogravimetric analysis, ^{1}H NMR and FTIR spectroscopy and transmission electron microscopy.

Published by Elsevier Ltd.

1. Introduction

Organic and inorganic nanoparticles are the building blocks in various nanotechnology applications [1]. One of the important applications of nanoparticles is their use as flow-modifiers for liquids and polymer melts. In 1906, Einstein demonstrated that the viscosity of a liquid increases upon addition of suspended Brownian particles [2]. Recently, contrary to Einstein's theory, Mackay and co-workers have shown that the melt viscosity of polystyrene can actually decrease upon addition of polymeric nanoparticles [3–5]. The dispersion of nanoparticles in polymer melt would help in tailoring the flow properties to suit to the needs of application. However, it is difficult to disperse nanoprticles in polymer melt without phase segregation. Thus, an appropriate surface-functionalization of the nanoparticles is essential to enhance dispersion in polymer melt [5]. The preparation of surface-functionalized polymeric nanoparticles in a precisely controlled way remains a daunting task [1,6,7]. Advances in this area are important to nanoscience because by controlling the size and the functionality of the nanoparticles it is possible to tailor the flow property of polymer melt and expand the arsenal of materials available for nanotechnology.

The synthesis of polymeric nanoparticles can be achieved by equipping polymers with polymerizable groups, followed by intramolecular cross-linking in dilute solution [8,9], or by cross-linking the shell or core of micelles obtained from a block copolymer in a selective solvent [10,11]. Another approach for the synthesis of polymeric nanomaterials is through the crosslinking of self-assembled block copolymers in the solid state [16,17]. The resulting nanoparticles have many potential applications [12–15].

Recently, Hawker et al. developed a method for making polystyrene nanoparticles using thermal crosslinking of benzocyclobutene-containing copolymers [4,18]. These copolymers contained low levels (1–30 mol%) of benzocyclobutene, and thus intramolecular cross-linking lead to the formation of nanoparticles containing substantial amounts of non-crosslinked comonomer, generally styrene. In this work we report an approach to synthesize tunable crosslinked polymer nanoparticles having both well-defined spherical shape and tunable surface chemistry through the use of benzocyclobutene-containing block copolymers. In our method, well-defined micelles composed of diblock copolymer containing poly(4-vinylbenzocyclobutene) (PVBCB) segments are

* Corresponding authors. Department of Chemistry, University of Tennessee, Knoxville, TN 37996, USA.
E-mail addresses: jimmymays@utk.edu (J.W. Mays), baskaran@utk.edu (D. Baskaran).

0032-3861/$ – see front matter Published by Elsevier Ltd.
doi:10.1016/j.polymer.2009.10.038

used as precursor for the synthesis of functional organic nanoparticles through core crosslinking and subsequent cleavage of poly(butadiene) (PB) corona segments (Scheme 1). We describe the efficiency of micellar approach in obtaining crosslinked spherical polymeric nanoparticles and its limitation in terms of producing soluble nanoparticles. The problem associated with the intermolecular agglomeration of nanoparticles arising from the polar surface functional groups is also discussed.

2. Experimental section

All chemicals were purchased from Aldrich Chemical Company, except 4-bromobenzocyclobutene (97%), which was generously donated by the Dow Chemical Company, USA. Dibutylmagnesium (1 M in heptane), 1,2-dibromoethane (99%), sodium (99%, lumps in kerosene), potassium (98%, chunks in mineral oil), calcium hydride (CaH_2), sodium hydroxide (97%, NaOH), Mg turnings (99.98%), methyltriphenylphosphonium bromide (98%), ammonium chloride (99.5%), sodium bicarbonate (99.7%), and *n*-butyllithium (1.6 M in hexane) were used as received. Benzene was freed from olefinic impurities by stirring over concentrated sulfuric acid for a week. This benzene was then stirred over CaH_2 and degassed, before distilling into a flask containing a small amount of *n*-BuLi and styrene connected to a vacuum line. Tetrahydrofuran (THF) was stirred over CaH_2 and degassed and stored on a vacuum line. THF was further purified by distillation in-vacuo into a flask containing Na/K (1:3) alloy. A bright blue color develops after stirring for some time due to solvated electrons and is indicative of high THF purity. Tetradecane, *n*-hexane, and decane were purified by distillation from a small amount of CaH_2 and further distillation from *n*-BuLi. Dimethylformamide (DMF) was distilled over NaOH. Other solvents such as ethyl acetate, diethyl ether and hexanes were used as received. 4-Bromobenzocyclobutene was distilled under vacuum and stored under N_2.

sec-Butyllithium (*s*-BuLi), synthesized by the reaction of *sec*-butyl chloride and lithium metal, was used as the polymerization initiator. The concentration of *s*-BuLi was determined by polymerizing a known quantity of styrene under high vacuum conditions, followed by measuring the number–average molecular weight of the polystyrene obtained at 100% conversion. 1,3-Butadiene was distilled from CaH_2 into a flask containing *n*-BuLi and stirred for an hour under vacuum at −10 °C. Then, the required amount of 1,3-butadiene was distilled into glass ampoules, diluted by distilling in *n*-hexane (twice the volume of diene), and sealed off using a torch. 4-Vinylbenzocyclobutene was synthesized from 4-carboxaldehydebenzocyclobutene as reported in the literature [18]. The monomer was purified by distillation from CaH_2 and from dibutylmagnesium, on the vacuum line and was then stored in ampoules. ^{1}H NMR (400 MHz, $CDCl_3$) δ 7.27 (d, 1H, ArH), 7.2 (s, 1H, ArH), 7.05 (d, 1H, ArH), 6.73 (dd, 1H, CH), 5.7 (d, 1H, $-CH_2-$), 5.2 (d, 1H, $-CH_2-$), 3.22 (s, 4H, $-CH_2-$) (Fig. 1i). ^{13}C NMR (100 MHz, $CDCl_3$) δ 145.89, 145.56, 137.74, 136.45, 125.56, 122.42, 119.70, 112.22, 29.35, and 29.19.

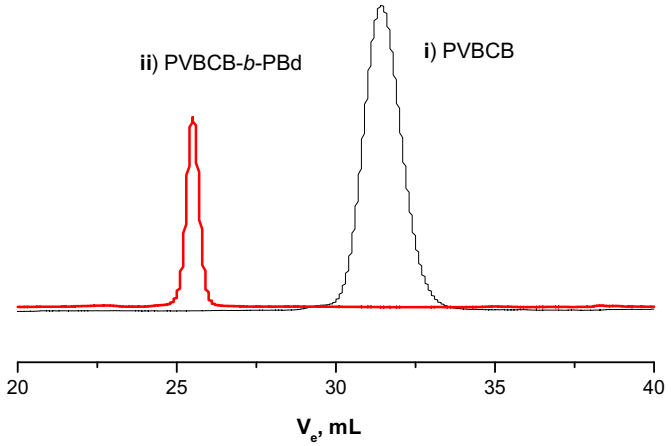

Fig. 1. SEC traces of PVBCB and PVBCB-*b*-PB ($M_{w,LS}$ = 23,000 g/mol, M_w/M_n = 1.02) synthesized using living anionic polymerization in benzene at 25 °C (Table 1, sample **4**).

2.1. Synthesis of poly(4-vinylbenzocyclobutene-b-butadiene)

The sequential block copolymerization of 4-vinylbenzocyclobutene and 1,3-butadiene was performed using standard all-glass high vacuum techniques, as described in our recent publication [19]. In a typical reaction, s-BuLi (0.001 mol) and 4-VBCB (2 g, 0.015 mol) were mixed in benzene (100 mL) at 30 °C and kept for 12 h. A small amount of sample was withdrawn into an empty ampoule and sealed off after washing the glass constriction with benzene condensed from the reaction mixture. Subsequently, 8 mL of 1,3-butadiene (6 grams in 15 mL hexane) was added through a break seal into the reactor containing living poly(4-vinylbenzocyclobutene) anions. Upon mixing of 1,3-butadiene, the orange color of the reaction medium become colorless, which indicated the initiation of 1,3-butadiene. In one of the reaction, a small amount of THF (~1 mL) was added to see the effect of polar solvent on the block copolymerization (Table 1, run 6). The polymerization was allowed to continue for 15 h at 25 °C and terminated with methanol (~0.5 mL) under vacuum. The reactor was opened and the block copolymer, poly(4-vinylbenzocyclobutene-*block*-butadiene), was precipitated in methanol and dried under vacuum at 40 °C for 24 h. The yield was 98% (~7.8 g). ^{1}H NMR (400 MHz, $CDCl_3$) δ 6.2–6.9 (ArH), 5.4 ($-CH{=}CH-$), 4.8 ($-CH{=}CH_2-$), 3.22 (cyclobutene, $-CH_2-$), 2.1 ($-CH_2-$) 1.6–2.2 ($-CH-$), 1.2–1.58 ($-CH_2-$).

2.2. Preparation of micellar solution and cross-linking

A required amount of the poly(4-vinylbenzocyclobutene-*block*-butadiene) diblock copolymer was dissolved in decane for the preparation of a stock solution. This solution was heated under an argon atmosphere at 75 °C overnight and was used to make

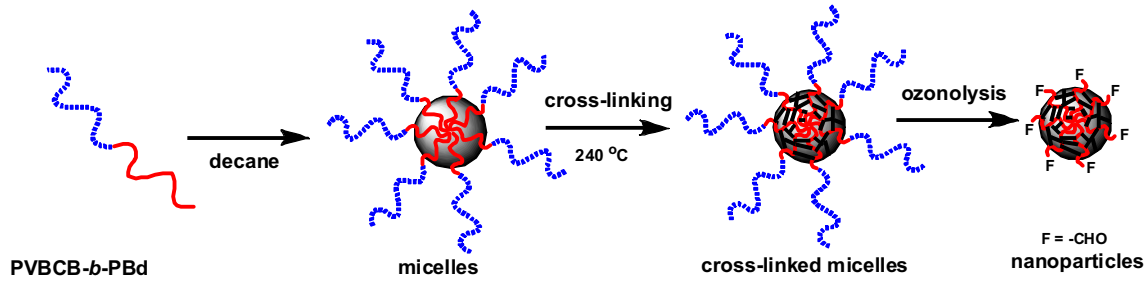

Scheme 1. Preparation of functionalized polymeric nanoparticles from micelles of poly(4-vinylbenzocyclobutene-b-butadiene) in tetradecane.

Table 1
Molecular characteristics of poly(4-vinylbenzocyclobutene-*b*-butadiene) (PVBCB-*b*-PB) diblock copolymers synthesized using sec-BuLi as initiator in benzene at 25 °C.

sample	$[s\text{-}BuLi] \times 10^3$ (mol/L)	$[M]_1$[a] (mol/L)	$[M]_2$[b] (mol/L)	$M_{n,th.}$[c] $\times 10^{-3}$(g/mol)	$M_{w,SEC\text{-}LS}$[d] (g/mol)	M_w/M_n[e]	mol% [f] PVBCB	%[g] 1,4-addition
1	10.00	0.15	1.10	8.0	9.0	1.01	21	89
2	5.38	0.27	0.61	12.0	12.0	1.01	56	90
3	6.88	0.42	1.02	16.0	15.0	1.03	50	90
4	2.75	0.23	0.67	24.0	23.0	1.02	39	90
5	2.66	0.30	0.74	30.0	32.0	1.03	50	87
6	1.25	0.38	0.93	80.0	74.0	1.09	47	61
7	5.00	0.23	1.29	20.0	19.0	1.07	44	89

[a] Concentration of 4-VBCB.
[b] Concentration of 1,3-butadiene.
[c] $M_{n,th}$ = gram of $(M_1 + M_2)$/[*s*-BuLi].
[d] Molecular weight determined using SEC-LS in tetrahydrofuran (THF) at 25 °C.
[e] Determined using SEC.
[f] Mol% of PVBCB using ^{1}H NMR in $CDCl_3$ (200 MHz).
[g] 1,4-addition of polybutadiene determined by ^{1}H NMR.

solutions of lower concentrations. All solutions had a characteristic blue tint attributed to the presence of micelles. Before light scattering experiments, the solutions were filtered through 0.45 μm pore size nylon filters. In a 500 mL four-necked flask equipped with internal thermometer, a condenser, an inlet for argon and a septum, 100 mL of tetradecane was heated to the desired temperature (200–240 °C) under argon. A micellar solution of the diblock copolymer in decane (3.2 g/100 mL), was added drop-wise into the hot tetradecane using a peristaltic pump at a rate of 30 mL/h with vigorous stirring under argon. After the addition, the reaction mixture was kept stirring for an additional 45 min. Subsequently, the solvent was distilled off under reduced pressure (vacuum line), and the remaining crude product was dissolved in THF and precipitated in excess methanol.

2.3. Cleavage of polybutadiene segments through ozonolysis

In a 500 mL two-necked flask equipped with a glass tube to introduce ozone, a calcium chloride drying tube, and a magnetic stirring bar, a solution of the crosslinked micelles (3 g) in dichloromethane (200 mL) was added. The solution was cooled to −78 °C, and ozone was bubbled through it at −78 °C under stirring, until the solution turned dark blue. After the reaction, the excess ozone was removed by purging with nitrogen for about 30 min. To this solution was added dimethyl sulfide (45 mL) at −78 °C, in order to quench the ozonide. The reaction mixture was then stirred at room temperature for 12 h. The solvent and the excess of dimethyl sulfide were distilled off under reduced pressure, and the remaining yellow solid was dried in vacuum.

2.4. Functionalization of the nanoparticles using PS-NH_2

The aldehyde-functionalized nanoparticles (sample run 3) were reacted with a 2-fold excess of primary amine terminated polystyrene (PS-NH_2, 4 K) in dry CH_2Cl_2/CH_3OH (1:1, v/v). The concentration of aldehyde groups was derived from N_{agg} assuming every nanoparticle has a minimum of 78 terminal groups after ozonolysis. The reaction was allowed to proceed for 7 days at room temperature with vigorous stirring (and sonication) under nitrogen to form the imine (Schiff base) derivative. A 5-fold excess of $NaBH_3CN$ (390 equiv based on the 78 functional groups) was added in five portions over 5 h. After the addition, the reaction mixture was refluxed for 6 h and concentrated under vacuum. Work-up consisted of the addition of 10% HCl to pH 5 with stirring overnight, filtration, and concentration. The residue was partitioned between saturated aqueous K_2CO_3 and CH_2Cl_2. The aqueous phase was extracted with CH_2Cl_2, and the organic phases were combined, dried with $MgSO_4$, and concentrated. The resulting product mixture was diluted in toluene and fractionated using CH_3OH as a non-solvent. The fractions were analyzed using size exclusion chromatography (SEC).

Details of characterization and instrumentations are given in supporting information.

3. Results and discussion

The synthesis of spherical surface-fuctionalized crosslinked nanoparticles using block copolymer micelles as precursor requires the use of a special diblock copolymer having both crosslinkable and cleavable segments that can self-assemble into micelles in a selective solvent. Poly(4-vinylbenzocyclobutene (PVBCB) and polybutadiene (PB) were selected as the segments for the diblock copolymer since the former can be thermally crosslinked and the latter can be cleaved through ozonolysis [20], leaving functional groups on the surface of the resulting nanospheres. The diblock copolymer, poly(4-vinylbenzocyclobutene-*b*-butadiene) (PVBCB-*b*-PB), self-assembles into micelles in decane, a selective solvent for PB (shell), with PVBCB as the core. Benzocyclobutene groups in the PVBCB micellar core are known to undergo thermal crosslinking via inter/intramolecular biradical reactions involving an *o*-quinodimethane intermediate [18,21]. Nanoparticles can thus be formed by crosslinking the micellar core and cleaving the 1,4-polybutadiene corona via ozonolysis. To accomplish this task, several diblock copolymers were synthesized through sequential living anionic polymerization under high vacuum (Table 1).

3.1. Synthesis of poly(4-vinylbenzocyclobutene-b-butadiene) (PVBCB-b-PB) diblock copolymer

Accordingly, living anionic polymerization of 4-vinylbenzocyclobutene was performed using *sec*-BuLi as initiator in benzene at room temperature. The polymerization proceeded in a controlled manner. Several PVBCBs, having measured molecular weights corresponding to the amounts of monomer and initiator used, were obtained with narrow molecular weight distribution. The living anions of PVBCB were used to initiate the polymerization of butadiene in benzene to form well-defined PVBCB-*b*-PB diblock copolymers. The orange color of the living PVBCB anions disappeared immediately upon addition of butadiene, indicating rapid initiation of butadiene. The reaction was continued for 15 h at 25 °C for complete monomer conversion. The diblock copolymers were characterized using Size exclusion chromatography (SEC) coupled with a light scattering detector. The diblock copolymers exhibited narrow molecular weight distributions with molecular weights (Table 1) that were close to stoichiometric values. Fig. 1 shows the SEC chromatograms of a PVBCB and a PVBCB-*b*-PB diblock

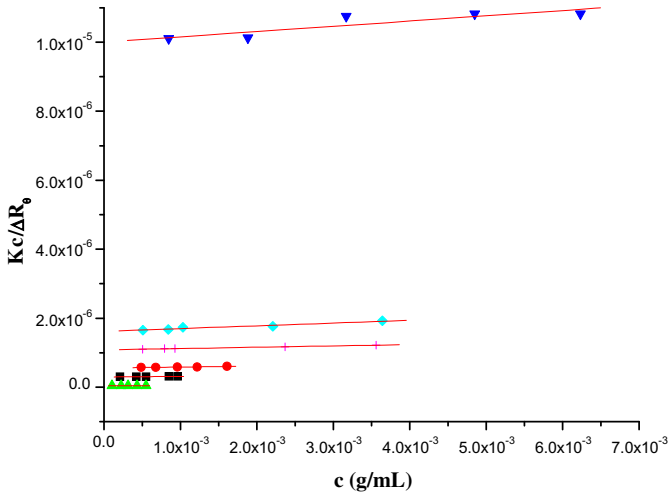

Fig. 2. Static light scattering plot of PVBCB-*b*-PB diblock copolymers in decane at 25 °C: Sample 1(■), Sample 2(●), Sample 3(▲), Sample 4(▼), Sample 5(◆), Sample 6(+).

copolymer synthesized using sequential anionic polymerization. Several diblock copolymers, with molecular weights ranging from 9000 g/mol to 74,000 g/mol, were synthesized. ^{1}H NMR analysis of the PVBCB-*b*-PB copolymers revealed that the mol% of PVBCB is in the range of 40 to 50%, except for a sample which was designed to have a low content of PVBCB (20.8 mol%, sample **1**). The sample 6 exhibited a low 1,4-content of PB segment due the presence of THF in the reaction. However, the formation of diblock in the presence of polar THF additive was incomplete, ~30% of homopolymer was terminated due to THF and the pure diblock copolymer was fractioned for further studies.

Thermogravimetry analysis (TGA) of the PVBCB-*b*-PB block copolymers exhibited two distinct steps of decomposition, at 360–480 °C (T_{max} = 455 °C) and at 500–580 °C (T_{max} = 566 °C). The major weight loss at 455 °C is a result of thermal decomposition of the polymer. At 200–240 °C, the benzocyclobutene moiety undergoes inter or intra molecular cross-linking in the solid state leading to the formation of a rigid network structure which decomposes at higher temperature (T_{max} = 566 °C) (Supporting Information). A slight weight increase was observed at 150 °C when the TGA experiment was conducted in air. This weight increase is attributed to the formation of radicals of the cyclobutene moiety and their rapid reaction with the oxygen present in the furnace, resulting in a slight weight gain before decomposition [19]. The differential scanning calorimetry (DSC) measurements were performed from room temperature to 150 °C at the heating rate of 5 °C per minute in order to examine the glass transition behavior of the PVBCB segments in the diblock copolymer. The diblock copolymers showed a transition at 119 °C corresponding to the T_g of PVBCB segments.

3.2. Characterization of micelles using SLS and DLS

The diblock copolymers were dissolved in decane, a thermodynamically good solvent for PB and a non-solvent for PVBCB, in order to form micelles. The solutions of PVBCB-*b*-PB diblock copolymer in decane exhibited a bluish tint due to scattering of light from the intermolecularly collapsed PVBCB segments. This observation is a visual evidence for the formation of micelles. The micelles were subjected to static and dynamic light scattering (SLS and DLS) and viscometry analyses. SLS measurements on the micellar solutions were performed over the concentration range of $10^{-4} < [C]_o < 7 \times 10^{-3}$ g/mL. This concentration range was particularly chosen based on the known behavior of diblock copolymers of polystyrene and polybutadiene in order to stay above the critical micelle concentration (cmc). Diblock copolymers of this type generally have a very low cmc and hence, the scattering intensity could be totally attributed to the self-assembled micelles. A plot of reduced scattering intensity with respect to concentration for all the diblock copolymer micelles in decane at 25 °C is shown in Fig. 2. Apparent weight–average molecular weights, $M_{w,app}$ of the micelles were determined from extrapolation to infinite dilution. The results obtained from SLS indicate very high molar masses for the micelles (Table 2). The apparent aggregation numbers (N_w) were determined from the ratio of the M_w of micelles in decane and the M_w of the diblock copolymer in THF, a common good solvent for both of the blocks ($N_w = M_{w,micelle}/M_{w,unimer}$).

The N_w values for the micelles were in the range of 11 to 326, depending on the composition of the diblock precursors. Since the micelle size depends on the total molecular weight and the insoluble block content, N_w increases with increasing molecular weight of the diblock and increasing segmental length of PVBCB [22–24]. The diblock copolymer with $M_{w,LS}$ = 74,000 g/mol (47% PVBCB) formed micelles with a very high N_w = 326 (Table 2, Sample 6). On the other hand, the diblock copolymer with 21% PVBCB (Table 2, sample **1**) with a low $M_{w,LS}$ = 9000 g/mol had a smaller, N_w = 11. The second virial coefficient, A_2 obtained from the slope of the plot in Fig. 2, decreases with increasing micellar size. The low values are in good agreement with the high association numbers of the micelles.

The DLS of these micelles showed the presence of slow diffusing particles. A plot of the concentration dependence of the diffusion coefficient is shown in Fig. 3a. The diffusion coefficients are very small reflecting a low mobility of the supramolecular structure in decane. As expected the values of the apparent diffusion coefficient, D_0 decrease with increasing molecular weight of the micelles. The

Table 2
Characterization of PVBCB-*b*-PB copolymer micelles in decene using SLS and DLS in *n*-decane at 25 °C.

Sample	% PVBCB[a]	$M_{w,app}$[b] × 10^{-6}	N_w[c]	R_g[d] (nm)	A_2 (mL mol g^{-2}) × 10^6	$D_{0,app}$ (cm^2/s) × 10^8	k_D (mL/g)	R_h[e] (nm)	R_{core}[f] (nm)	L corona ($R_h - R_{core}$)	R_g/R_h
1	20.8	0,101	11	4.1	96.4	32.2	11.9	7.9	2.4	5.5	0.52
2	55.5	0,607	50	10.3	28.1	16.0	7.6	15.9	6.5	9.4	0.65
3	50.2	0,923	62	13.5	17.7	13.0	7.6	19.5	7.1	12.4	0.69
4	39.0	1,796	78	15.7	13.2	10.5	8.0	24.1	7.9	16.2	0.65
5	49.9	3,386	105	23.9	9.1	7.4	10.64	34.2	10.9	23.3	0.70
6	47.2	24,150	326	60.5	0.9	3.4	15.1	75.6	20.5	55.1	0.80

[a] Using ^{1}H NMR in $CDCl_3$ (200 MHz).
[b] Weight average molecular weight of the micelles measured by SLS in decane at 25 °C.
[c] $N_w = (M_{w,LS\text{-micelles}})/(M_{w,LS\text{-diblock}})$.
[d] R_g determined by LS (Zimm plot).
[e] Measured by DLS in decane at 25 °C.
[f] Calculated using, $R_c = (3\ M_{w,micelles}.wt._{(PVBCB)}/4\pi N_A d_{(PVBCB}.\varphi\}^{1/3}$ where theoretical density is 0.3 g/mL [29] and $\varphi = 1$ for dry core in decane and $\varphi = 0.5$ for swollen core in THF.

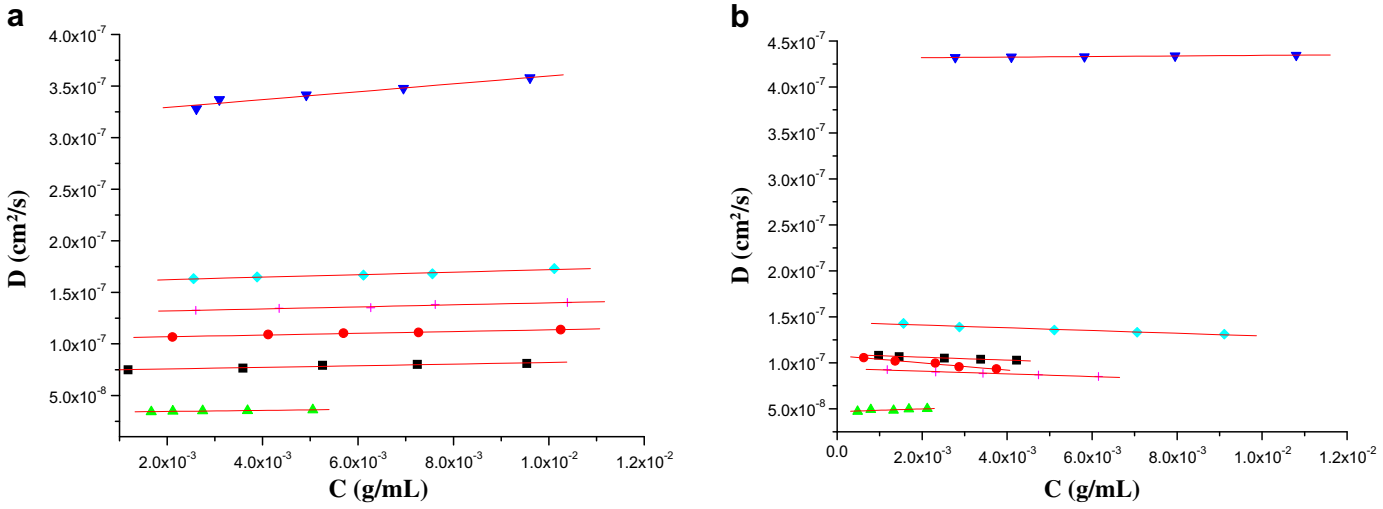

Fig. 3. Diffusion coefficient with respect to concentration for micelles of PVBCB-*b*-PB in decane before (a) and after (b) crosslinking the core at 25 °C: sample 1(■), sample 2(●), sample 3(▲), sample 4(▼), sample 5(◆), sample 6(+).

concentration dependent diffusion coefficient, k_D values show no specific trend with M_w of the micelles. However, the low values of k_D may be related to the predominance of hydrodynamic friction factors over thermodynamic ones as well as due to the low A_2 values obtained for these micelles.

The hydrodynamic radii (R_h) of the micelles determined from the D_o values using the Stokes–Einsten equation were in the range of 8–76 nm and increase with increasing M_w of the diblock and increasing N_w of the micelles (Table 1 and 2, Fig. 4). The spherical nature of the micelles was confirmed by the ratio of relaxation rate (Γ) of the correlation function to scattering vector (q^2), a characteristic line width (Γ/q^2), which exhibited no angular dependence. The polydispersity index, expressed by the ratio μ_2/Γ^2 via cumulant analysis, is ≤0.12 in all cases, revealing that the micelles formed are near-monodisperse in size. The size of the core for these micelles can be calculated using Eq. (1).

$$R_c = (3M_{w,micelles} wt_{\cdot(PVBCB)}/4\pi N_A d_{(PVBCB)}\varphi)^{1/3} \quad (1)$$

where $M_{w,micelles}$ is the molecular weight of micelles in decane, N_A is Avogadro's number, $wt_{\cdot(PVBCB)}$ is the weight fraction of the core forming block (PVBCB), and $d_{(PVBCB)}$ is the theoretical density, 0.3 g/mL [29] and $\varphi = 1$ for dry core in decane and $\varphi = 0.5$ for swollen core in THF. The size of the core increases with increasing N_w and $M_{w,app}$ (Table 2).

The ratio of R_g/R_h is in the range of 0.65 which is consistent with the presence of a densely collapsed PVBCB core exhibiting a smaller core-size (R_{core}) (2.4 nm < R_{core} < 20.5 nm) (Table 2) [25]. The ratio R_g/R_h gives information about the morphology of the micelles, which depends on the branching density, polydispersity, and the inherent flexibility of the subchains and is a sensitive fingerprint of the inner density profile. For an uniform non-draining solid sphere, the ratio is 0.774 [25]. The above ratio for most of the micelles in decane is in the range of 0.65–0.70, a typical value for polymeric micelles since the density of the core is much larger than that of the shell. These structures can be described as soft spherical structures. Samples **6** and **1** gave a high R_g/R_h ratio of about 0.80 and a very low values ($R_g/R_h = 0.52$) respectively, which can be attributed to a high and a very low association number of these structures, respectively (Table 2).

To further confirm the results obtained from the light scattering measurements, the solution properties of these micelles were explored using viscometry in decane at 25 °C. The viscometry results are presented in Table 3, and representative Huggins and Kraemer plots for the micelles, derived from a PVBCB-*b*-PB with $M_{wLS} = 1.79 \times 10^6$ g/mol, are shown in Fig. 5 (Table 3, sample **4**). The intrinsic viscosity, [η], values are low considering the high molecular weight of the micelles, which also confirms the compact structure of these materials. The k_H values are large ($k_H > 1.0$) as compared to typical values for random-coil polymers in good solvents. This can be attributed to the presence of an enhanced intramolecular hydrodynamic interaction within the micelles. In almost all cases the k_H values are higher than the theoretical value for hard spheres ($k_H = 0.99$) indicating again a highly compact spherical structure of these micelles. The only sample that has a k_H value much lower is sample **1** and this could be due to the very low aggregation number ($N_w = 11$). The viscometric radii, R_v, were calculated from Eq. (2) and the values are reported in Table 3. The ratio R_v/R_h is around 0.7 for most of the micelles. Although, it is expected that the ratio should be close to unity for a compact spherical micelles, the deviation from unity can be explained on the basis that the micelles in a capillary tube experience shear forces that may sometime disrupt the micelles partially, leading to lower R_v values.

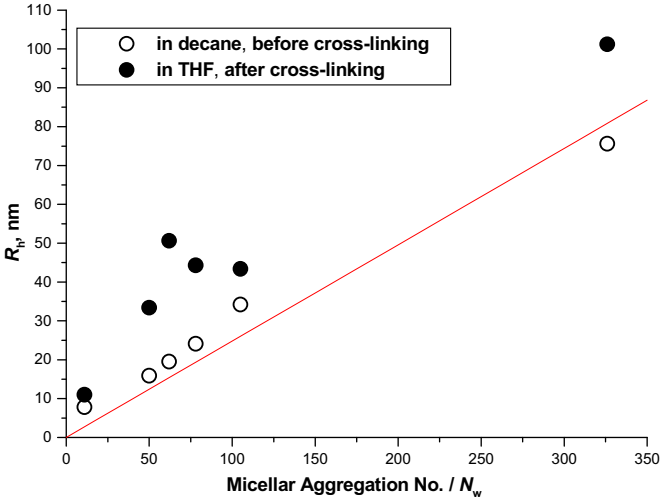

Fig. 4. Hydrodynamic radius of the PVBCB-*b*-PB micelles in tetradecane before crosslinking the core and core crosslinked micelles in good solvent (THF).

Table 3
Viscometry results for the PVBCB-*b*-PB diblock copolymers in *n*-decane at 25 °C.

Sample	$[\eta]$ (dL/g)	k_H	R_v[a] (nm)	R_v/R_h
1	0.1674	0.55	6.4	0.81
2	0.1197	1.02	10.5	0.67
3	0.1357	1.23	12.6	0.65
4	0.1988	1.22	17.8	0.74
5	0.1914	1.01	21.7	0.64
6	0.2907	1.75	48.1	0.64

[a] Calculated from Eq. (2).

$$R_v = (3/10.\,\pi.N_A)^{1/3}\,([\eta]M_{w,app})^{1/3} \quad (2)$$

where $M_{w,app}$ is the weight-average molecular weight determined by light scattering measurements.

3.3. Crosslinking of micelles

The stock solutions of the micelles prepared in decane were used for crosslinking at high temperature in tetradecane following Hawker's procedure [18]. Accordingly, the micelle solution in decane was added drop-wise (30 mL/h) into tetradecane at 240 °C and the solution was kept stirring for an additional 45 min. The drop-wise addition of micelles into tetradecane at 240 °C was expected to minimize dissociation of micelles into unimers at high temperature. The crosslinking reactions were also performed at different temperatures to understand the crosslinking efficiency. The core crosslinked micelles were recovered after removing solvent by vacuum distillation and precipitation in excess methanol. If the micelles are crosslinked at the core, their structure would be intact and they may be dispersed in non-selective solvents (i.e. good solvents for both blocks) without dissociation into unimers. Accordingly, the core crosslinked micelles were dissolved in THF and examined using SEC. All the core crosslinked micelles dissolved smoothly in THF. This confirms that the crosslinking reaction took place only in side the core of micelles without forming network or gel.

The SEC traces of core crosslinked micelles in THF revealed a substantial shift to a lower elution volume compared to that of the diblock copolymer, thus they are structurally intact confirming the formation of stabilized micelles. The polydispersity indices of the core crosslinked micelles were moderately narrow ($1.3 < M_w/M_n < 1.5$) and free from unimer when the crosslinking is performed at higher temperature at 240 °C (Fig. 6). The presence of a shoulder on the low molecular weight side of the SEC trace is attributed to the formation of smaller micelles, relative to the initial micelles, resulting from partial dissociation of micelles at high temperature during crosslinking. The dissociation of micelles into unimers at levels up to about 10–15% was detected when the crosslinking was performed at 200 °C (Fig. 6a). Hence, it is essential to perform the cross-linking at higher temperature (240 °C) to minimize the dissociation of micelles. The crosslinking at 240 °C showed no unimer signals in the SEC traces (Fig. 6b) indicating the micelles are kept intact through radical crosslinking. The temperature dependent nature of the crosslinking reaction suggests that it is possible to obtain partially cross-linked micelles. The crosslinking was also confirmed by DSC analysis showing a disappearance of T_g at ~120 °C corresponding to the PVBCB block after the crosslinking reaction (Fig. 7).

The DLS analysis of the core crosslinked micelles in THF, a good solvent for both blocks, indicated the presence of micelles, confirming the intactness of the micellar structure (Table 4). This confirms that the micelles in fact underwent crosslinking reaction at high temperatures. Apparent diffusion coefficients, $D_{o,app}$ of the core crosslinked micelles do not follow any trend with respect to the molecular weight of the micelles. This could be due to the presence of intermediate crosslinked micelles. The R_h and the R_{core} of core crosslinked micelles in THF were slightly higher as compared to those before crosslinking (Fig. 3b and Fig. 4). This increase can be attributed to the swelling of the crosslinked core in THF, which is a good solvent for both PB and PVBCB. Viscosities of

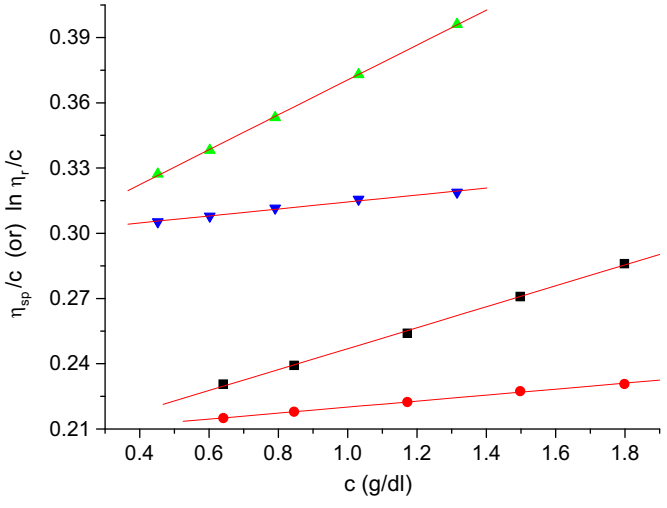

Fig. 5. Huggins (■) and Kraemer (●) plots for micelles derived from PVBCB-*b*-PB diblock copolymer, **4** in decane and plots for core crosslinked micelles of diblock copolymer, **4** in THF (Huggins (▲) and Kraemer (▼)).

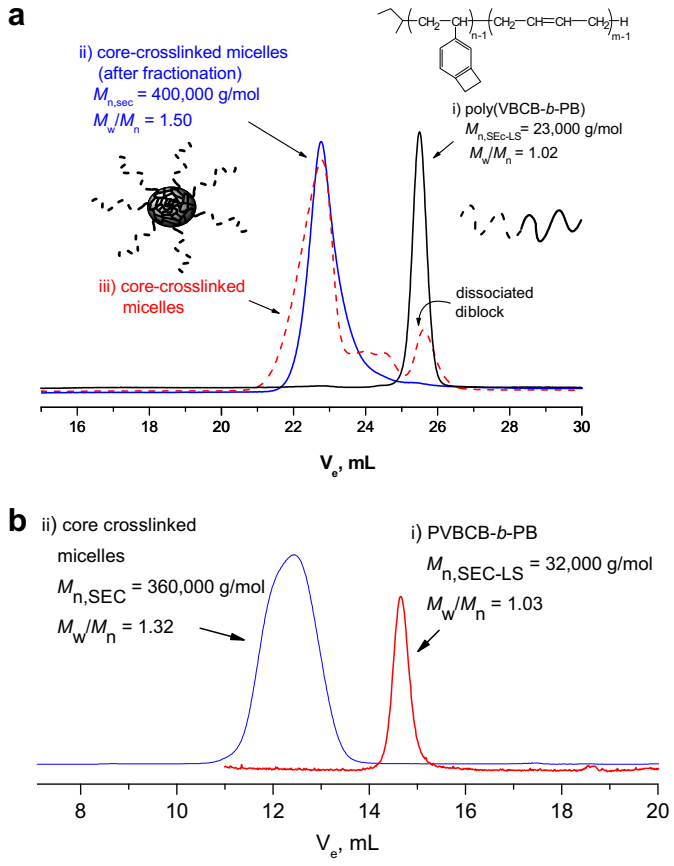

Fig. 6. SEC traces of core crosslinking reaction for PVBCB-*b*-PB copolymers: a) reaction performed at 200 °C; sample **4** and b) reaction performed at 240 °C; sample **5**.

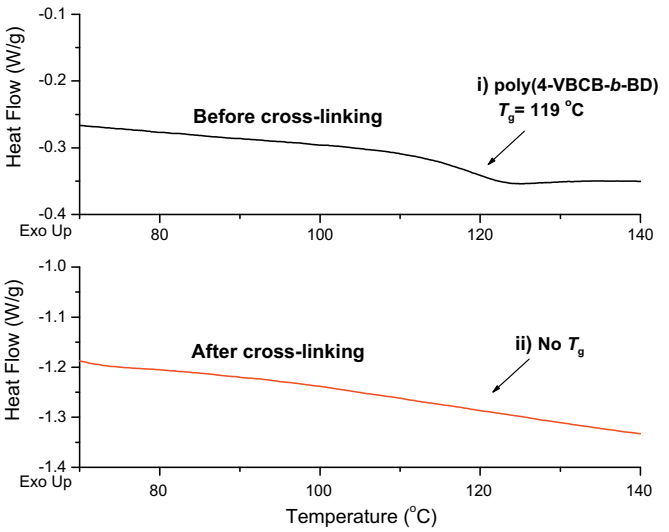

Fig. 7. Reversible heat capacity vs temperature plots showing i) the T_g of the PVBCB block at 120 °C, and ii) no T_g was observed in core cross-linked micelles (sample **4**) over the temperature range investigated.

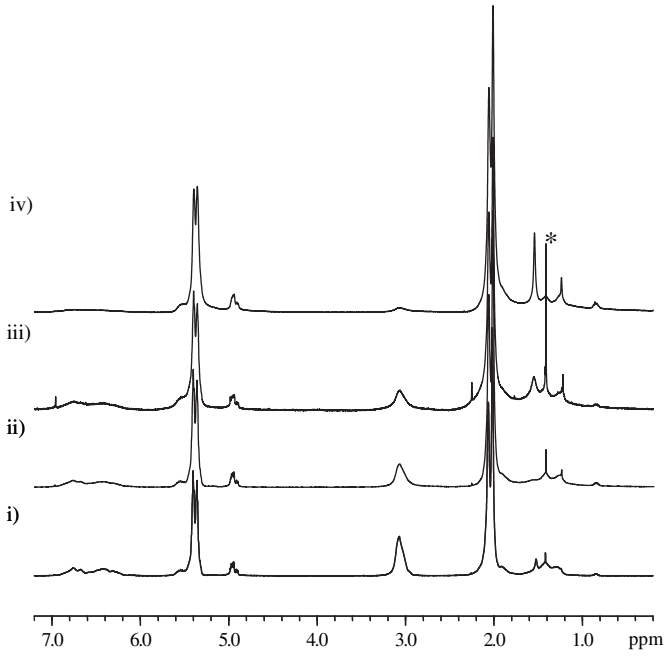

Fig. 8. ^{1}H NMR spectra of block copolymer micelles in $CDCl_3$; i) diblock copolymer **2** in Table 1,ii) micelles after crosslinking at 200 °C, iii) micelles after cross-linking at 220 °C, and iv) micelles after cross-linking at 240 °C (* corresponds to residual moisture in $CDCl_3$).

the core crosslinked micelles show a substantial increase as compared to the precursor micelles (Fig. 5).

The evidence for the formation of core crosslinked micelles also came from the disappearance of the ^{1}H NMR signals corresponding to the cyclobutene moiety at 3.15 ppm in the core crosslinked micelles in $CDCl_3$ (Fig. 8, iv). It was noticed that the intensity of the cyclobutene signal at 3.15 ppm decreases gradually with increasing temperature of the crosslinking reaction. However, the ^{1}H NMR signals of the dimerized *o*-quinodimethane in the core crosslinked micelles are not at all seen in the crosslinked micelles (Scheme 2). This could be due to presence of high concentration of benzocyclobutene in the core leading to several radical side reactions. Harth et al. showed that the signals associated with the dimerized *o*-quinodimethane through bi-radical coupling reaction during the crosslinking appear at ~2.8 ppm in the intramolecularly collapsed nanoparticle prepared from statistical copolymers of styrene and 4-vinyl benzocyclobutene [18]. On the other hand, there are new signals appearing at 0.9, and 1.56 ppm whose intensities increase with increasing crosslinking temperature. It is also noticed that upon crosslinking all the signals become broad. It thus appears that the intermediate *o*-quinodimethane radicals also undergo side reactions in addition to dimerization. It should also be noted that the reaction of bromobenzocyclobutene with polystyrene homopolymer produced polystyrene copolymer containing bromobenzocylobutene attached on some of the phenyl rings through [4 + 2] cycloaddition (Supporting Information). Recently, we have used such a Diels-Alder reaction to functionalize multi-walled carbon nanotubes [26]. Several others have also used benzocyclobutene moiety for crosslinking of macromolecules [11,15,27,28].

$$(R_h = kT/6\pi.\eta_s.D_{o,app}) \quad (3)$$

where, k is the Boltzmann's constant, T is absolute temperature, and η_s is the viscosity of the solvent.

In order to understand the crosslinking chemistry of benzocyclobutene, a model reaction on the thermal dimerization of benzocyclobutene was carried out in bulk at 240 °C for 4 h under vacuum. The ^{1}H NMR of the crude product mixture showed signals corresponding to dimerization as well as oligomerization of *o*-quinodimethane (Scheme 2). The product mixture had multiplets at 2.8–3.1 ppm which could be assigned to dimerization product

Table 4
Dynamic light scattering and viscometric results from the THF solutions at 25 °C after crosslinking BCB moieties at the core of the micelles.

Sample	$D_{t,o} \times 10^8$[a] (cm^2/s)	k_D[b] (mL/g)	R_h[c] (nm)	R_{core}[d] (nm)	L corona ($R_h - R_{core}$)	$[\eta]$[e] (dL/g)	k_H[f]
1	43.11	0.8	11.0	3.0	8.0	0.1876	0.56
2	14.4	−10.53	33.0	8.2	24.8	0.1612	0.67
3	9.38	−15.7	50.6	9.0	41.6	0.1796	0.97
4	10.77	−36.3	44.1	10.0	34.1	0.2903	0.95
5	10.93	−14.54	43.4	13.8	29.6	0.2630	0.68
6	4.68	31.43	101.2	25.8	75.6	0.6259	1.39

[a,b] By DLS in *n*-decane at 25 °C.
[c] Calculated from Stokes–Einstein Eq. (3).
[d] Calculated from Eq. (1).
[e,f] By viscometry in *n*-decane at 25 °C.

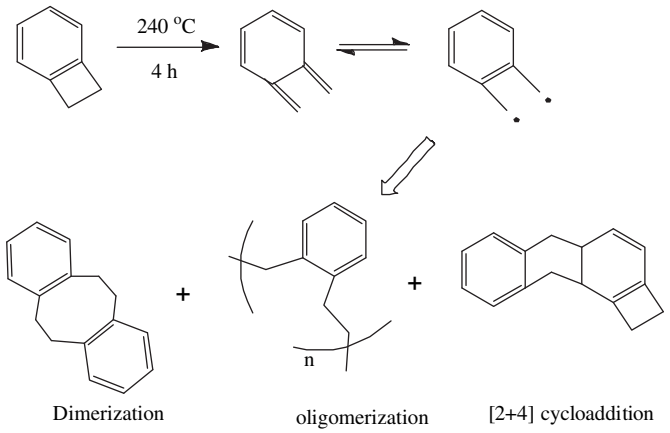

Scheme 2. Thermal crosslinking of benzocyclobutene in bulk at 240 °C through an *o*-quinodimethane radical intermediate and various modes of reactions.

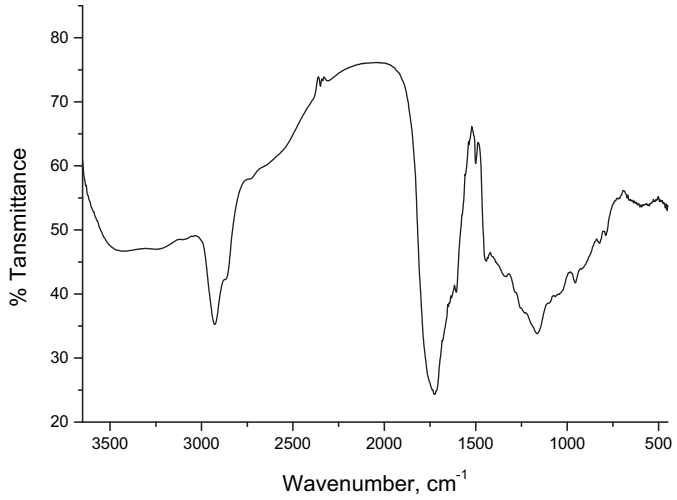

Fig. 9. FT-IR spectrum of functional organic nanoparticles showing signals corresponding to aldehyde (1740 cm^{-1}), and residual oligobutadiene fragments (2927 cm^{-1}).

and signals centered at ~0.9, ~1.6, and ~2.2 ppm along with olefin signals at ~5.6 and ~6.0 ppm could be attributed to the formation of linear oligomeric product through radical propagation of *o*-quinodimethane (Supporting information). The oligomer could be isolated as a viscous material through coagulation using methanol. The crosslinked micelles do show signals at 0.9 and 1.56 ppm, along with backbone methyl and methylene signals. The new signals could be attributed to crosslinking through linear oligomerization (Fig. 8-iv). It appears that crosslinking at the core of the micelles which occurs in the solid state does proceed through linear oligomerization process. The restriction of rotational freedom of benzocylobutene groups in the solid state might favor crosslinking through intermolecular oligomerization. Another problem associated with identification of such reactions in micelles is the difficulty in accessing the core component in NMR spectroscopy. It was observed that the ratio of methylene protons of cyclobutene to aromatic signals decreases with increasing reaction temperature. This confirms that the core of the micelles is not fully accessible to the ^1H NMR analysis due to crosslinking induced insolubility of the micelle core. In fact, when the crosslinking was performed at the higher temperature (240 °C), the signals corresponding to the aromatic and cyclobutene protons are significantly suppressed. This can be attributed to the insoluble nature of the crosslinked core in $CDCl_3$ after crosslinking. On the other hand, for crosslinking performed at lower temperatures, such as 200 and 220 °C, aromatic and cyclobutene signals can be seen due to reduced crosslinking (Fig. 8-ii, iii).

3.4. Preparation of nanoparticles through ozonolysis cleavage of PB corona segments of the micelles

In order to obtain functional nanoparticles, the core crosslinked micelles were subjected to ozonolysis to cleave the 1,4-polybutadiene corona segments in dichloromethane at −78 °C. The reaction mixture was subsequently quenched with dimethylsulfide, a reducing agent, to produce aldehyde functional groups on the surface of the nanoparticles. During the ozonolysis, the nanoparticles separated out as a pale yellow colored solid. Since they are densely crosslinked at the core, the nanoparticles became increasingly insoluble during the progression of ozonolysis. The insolubility causes a small amount of short oligobutadiene segments remains intact on the surface due to partial cleavage, as evident from the TGA analysis (discussed below). The nanoparticles obtained are insoluble in all solvents tested and agglomerate to form clusters. The FT-IR spectra of the nanoparticles show transmittance at 1740 cm^{-1}, 2830 cm^{-1}, and 2927 cm^{-1} confirming the presence of carbonyl aldehyde, –CH– (aldehyde), and $–CH_2–$ (oligobutadiene), respectively (Fig. 9). The presence of $–CH_2–$ groups is attributed to residual oligobutadiene segments attached to the surface of the nanoparticles and in part to $–CH_2–$ groups that are penultimate to the aldehyde groups on the nanoparticle surface.

The low solubility and agglomeration of the prepared nanoparticles is believed to be due to high level of crosslinking and the agglomeration through dipolar interactions between the aldehyde carbonyls. The nanoparticles decompose in air in multiple steps from 180 to 600 °C (Supporting Information). The initial decomposition from 180 to 400 °C can be attributed to several factors such as a) the presence of residual high boiling solvent (DMSO), b) the entrapment of fragmented oligobutadiene on the nanoparticles, c) the short hairy oligobutadiene segments on the surface of the nanoparticles resulting from incomplete ozonolysis and d) the decomposition of polar functional groups on the surface of the nanoparticles (Supporting Information). The incomplete nature

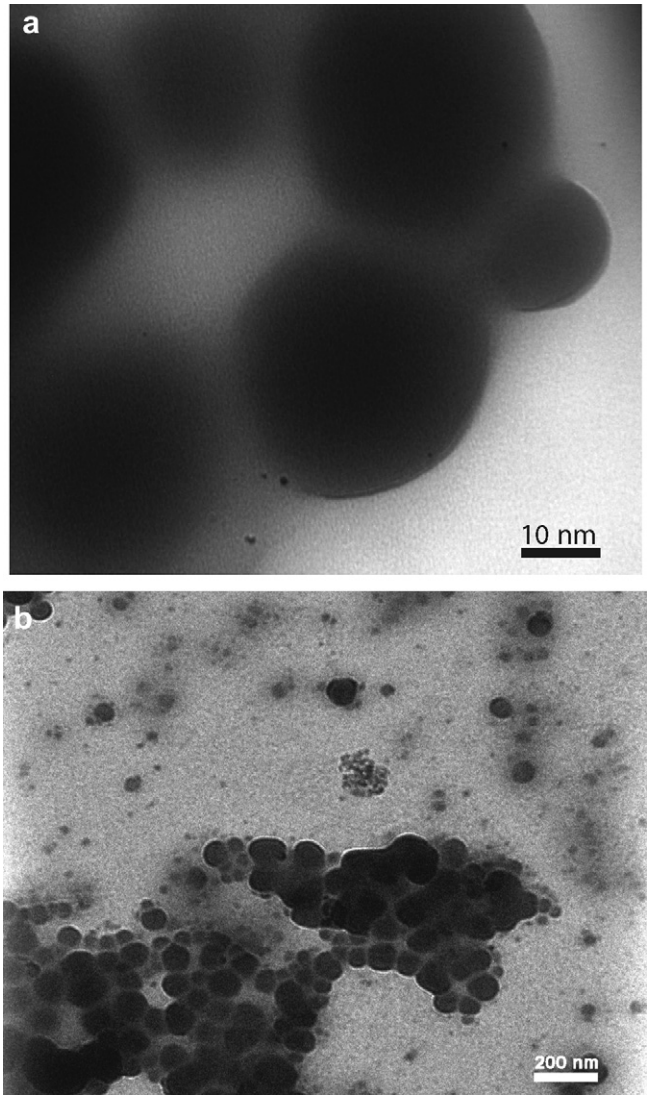

Fig. 10. TEM of individual (a) and agglomerated nanoparticles (b) prepared from PVBCB-*b*-PB micelles as precursor. The expanded region (a) shows presence of individual particles (Table 2, sample **4**).

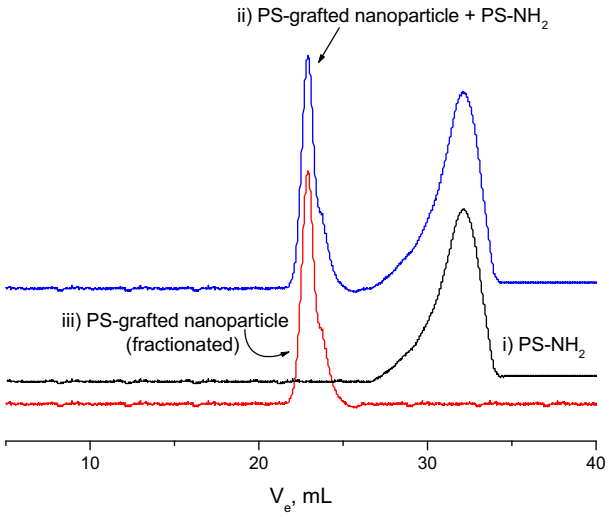

Fig. 11. SEC traces of oligostyrene grafted nanoparticles. i) precursor amine terminal oligopolystyrene (PS-NH_2) with $M_{n,app} = 4000$ g/mol and $M_w/M_n = 1.4$, ii) reaction product consisting of PS-grafted nanoparticles along with excess PS-NH_2, and iii) fractionated PS-grafted nanoparticles.

of the ozonolysis is attributed to the progressive insolubility of the nanoparticles during the reaction. However, the nanoparticles could be dispersed in a methanol/dimethylformamide mixture solvent under a mild sonication. The dispersion is not stable and agglomeration takes place immediately upon ceasing of sonication. A drop of the dispersed solution was coated immediately on a carbon grid for TEM characterization. TEM images show discrete nanoparticles ranging from ~16–20 nm with agglomerated nanoparticles ranging from ~30–100 nm in diameter with broad distribution (Fig. 10). Enlarged images of the agglomerated particles clearly show they are composed of individual nanoparticles. The size of the discrete nanoparticles is not comparable to that of the core-size of the diblock copolymer micelles, indicating clearly a strong agglomeration of nanoparticles. The agglomeration of nanopartilces could be attributed to various factors such as the presence of polar functional groups, changes in surface area, and partial swelling of segments as a result of incomplete ozonolysis.

Functional group modification is the best way to be able to re dissolve these particles in solvents. Accordingly, we decided to functionalize the nanoparticles through their aldehyde groups. The aldehyde groups present on the surface of the nanoparticles were reacted with telechelic oligostyrene bearing primary amine terminals (PS-NH_2, $M_{n,app}$ ~4000 g/mol, $M_w/M_n = 1.4$). The precursor oligomer used apparently exhibited a somewhat broad molecular weight distribution, which may be an artifact attributed to the NH_2 groups interacting with the SEC column material. The attachment of short PS chains on the nanoparticles should aid in dissolution of these nanoparticles in organic solvents and they should allow them to be easily dispersed in polystyrene melts.

The reaction was performed in dry CH_2Cl_2/CH_3OH (1:1, v/v) in the presence of excess sodium cyanoborohydride ($NaBH_3CN$), as a reducing agent for reductive alkylation under refluxing for 7 days. The resulting product showed an additional peak at higher elution volume in SEC analysis indicating the formation of oligostyrene grafted nanoparticles (Fig. 11). Since the reaction was performed with excess PS-NH_2, the presence of residual PS-NH_2 is also seen in the SEC trace (Fig. 11 ii). The PS-grafted nanoparticles were fractionated in toluene, which yielded a very high molecular weight product with a narrow molecular weight distribution (Fig. 11-iii). The opportunity for post-functionalization using different moieties allows for tailoring the dispersibility/solubilization of the nanoparticles in different media.

4. Conclusion

The synthesis of spherical surface-functionalized organic nanoparticles has been accomplished using reactive diblock copolymer micelles as precursor. Well-defined PVBCB-*b*-PB diblock copolymers were prepared using living anionic polymerization, and micelles of these diblock copolymers were formed in decane. The block copolymers and micelles were thoroughly characterized using SEC, ^{1}H NMR, dynamic and static light scattering and viscosity measurements. Thermal crosslinking of benzocyclobutene pendants at the core of the micelles was accomplished at different temperatures. The ^{1}H NMR of the cross-linked micelles at different temperature revealed the extent of crosslinking at the core, and the percentage of the unimer formation were found to be dependent on the temperature of the crosslinking reaction, hence, rendering a mechanism for control over the distribution and density of nanoparticles. Ozonolysis of the cross-linked micelles produced insoluble nanoparticles with aldehyde functional groups at the surface. The presence of functional group on the surface of the nanoparticles was confirmed by FT-IR. The synthesized nanoparticles were insoluble due to polar functional groups and high crosslinking. The TEM results indicated that the particles obtained were much higher in diameter as compared to precursor micellar core. Post-reaction with oligostyrene bearing primary amine terminals produced soluble oligostyrene grafted nanoparticles.

Acknowledgment

We acknowledge U. S. Department of Energy (DE-AC05-00OR22725) for financial support.

Appendix. Supplementary data

Details of characterization, SEC traces of various core crosslinked diblock copolymer micelles, ^{1}H NMRs of thermal dimerization of benzocyclobutene at 240 °C and modified polystyrene using [4+2] cycloaddition with 1-bromobenzocylobutene, TGA of surface functionalized nanoparticles and additional TEM of nanoparticles. Supplementary data associated with this article can be found in the on-line version, at doi:10.1016/j.polymer.2009.10.038.

References

[1] Schmid G. Nanopartilces: from theory to application. Weinheim: Wiley-VCH; 2004.
[2] Einstein A. Ann Phys (Leipz) 1906;19:371.
[3] Mackay ME, Dao TT, Tuteja A, Ho DL, Horn BV, Kim H, et al. Nat Mater 2003;2:762.
[4] Tuteja A, Mackay ME, Hawker CJ, Van Horn B, Ho DL. J Polym Sci Part B: Polym Phys 2006;44:1930.
[5] Mackay ME, Tuteja A, Duxbury PM, Hawker CJ, Van Horn B, Guan ZB, et al. Science 2006;311:1740.
[6] Cuenya BR, Baeck SH, Jaramillo TF, McFarland EW. J Am Chem Soc 2003;125:12928.
[7] Scott RWJ, Sivadinarayana C, Wilson OM, Yan Z, Goodman DW, Crooks RM. J Am Chem Soc 2005;127:1380.
[8] Mecerreyes D, Lee V, Hawker CJ, Hedrick JL, Wursch A, Volksen W, et al. Adv Mater 2001;13:204.
[9] Jiang J, Thayumanavan S. Macromolecules 2005;38:5886.
[10] Cheng C, Khoshdel E, Wooley KL. J Am Chem Soc 2006;128:6808.
[11] Kim E, Shin C, Ahn H, Ryu DY, Bang J, Hawker CJ, et al. Solf Matter 2008;4:475.
[12] Zhang Q, Remsen EE, Wooley KL. J Am Chem Soc. 2000;122:3642.
[13] Turner JL, Chen Z, Wooley KL. J Control Release 2005;109:189.
[14] Ryu DY, Shin K, Drockenmuller E, Hawker CJ, Russell TP. Science 2005;308:236.
[15] So Y-H, Foster P, Im J-H, Garrou P, Hetzner J, Stark E, et al. J Polym Sci: Part A: Polym Chem 2006;44:1591.
[16] Yan X, Liu G, Li Z. J Am Chem Soc 2004;126:10059.

[17] Drockenmuller E, Li LYT, Ryu DY, Harth E, Russell TP, Kim H-C, et al. J Polym Sci Part A: Polym Chem 2005;43:1028.
[18] Harth E, Horn BH, Lee VY, Germack DS, Gonzales CP, Miller RD, et al. J Am Chem Soc 2002;124:8653.
[19] Sakellariou G, Baskaran D, Hadjichristidis N, Mays JW. Macromolecules 2006;39:3525.
[20] Criegee R. Angew Chem Int Ed Engl 1975;14:745.
[21] Deeter GA, Venkataraman D, Kampf JW, Moore JS. Macromolecules 1994;27:2647.
[22] Qin A, Tian M, Ramireddy C, Webber SE, Munk P. Macromolecules 1994;27:120.
[23] Halperin A, Tirrell M, Lodge TP. Adv Polym Sci 1992;100:31.
[24] Iatrou H, Willner L, Hadjichristidis N, Halperin A, Richter D. Macromolecules 1996;29:581.
[25] Burchard W. Adv Polym Sci 1999;143:113.
[26] Sakellariou G, Ji H, Mays JW, Hadjichristidis N, Baskaran D. Chem Mater 2007;19:6370.
[27] Blomberg S, Ostberg S, Harth E, Bosman AW, Horn B, Hawker CJ. J Polym Sci, Part A: Polym Chem 2002;40:1309.
[28] So Y-H, Hahn SF, Li Y, Reinhard MT. J Polym Sci, Part A: Polym Chem 2008;46:2799.
[29] Bicerano J. Prediction of polymer properties. 2nd ed. Marcel Dekker Inc; 1996.